Received: 30 January 2020 | Revised: 15 September 2020 | Accepted: 1 October 2020

DOI: 10.1111/aas.13723

acta Anaesthesiologica Scandinavica

ORIGINAL ARTICLE

Estimation of changes in cyclic lung strain by electrical impedance tomography: Proof-of-concept study

Rodrigo Cornejo[1,2] | Pablo Iturrieta[3] | Tayran M. M. Olegário[4] | Carolina Kajiyama[5] | Daniel Arellano[1,6] | Dannette Guiñez[1] | María A. Cerda[1] | Roberto Brito[1] | Abraham I. J. Gajardo[1] | Marioli Lazo[1] | Lorena López[7] | Caio C. A. Morais[8] | Sedric González[1] | Miguel Zavala[1] | Verónica Rojas[1] | Juan N. Medel[1] | Daniel E. Hurtado[3,9] | Alejandro Bruhn[10,2] | Cristobal Ramos[7] | Nivia Estuardo[1]

[1]Unidad de Pacientes Críticos, Departamento de Medicina, Hospital Clínico Universidad de Chile, Santiago, Chile

[2]Center of Acute Respiratory Critical Illness (ARCI), Santiago, Chile

[3]Department of Structural and Geotechnical Engineering, School of Engineering, Pontificia Universidad Católica de Chile, Santiago, Chile

[4]Escola Politécnica, Universidade de Sao Paulo, Sao Paulo, Brazil

[5]Development Division, Timpel SA, São Paulo, Brazil

[6]Departamento de kinesiología, Facultad de Medicina, Universidad de Chile, Santiago, Chile

[7]Departamento de Radiología, Hospital Clínico Universidad de Chile, Santiago, Chile

[8]Divisao de Pneumologia, Faculdade de Medicina, Instituto do Coracao, Hospital das Clinicas HCFMUSP, Universidade de Sao Paulo, Sao Paulo, Brazil

[9]Institute for Biological and Medical Engineering, School of Engineering, Pontificia Universidad Católica de Chile, Santiago, Chile

[10]Departamento de Medicina Intensiva, Facultad de Medicina, Pontificia Universidad Católica de Chile, Santiago, Chile

Correspondence
Rodrigo Cornejo, Universidad de Chile, Santos Dumont 999, Independencia, Santiago, Chile.
Email: racornej@gmail.com; rcornejor@hcuch.cl

Funding information
Supported by the grant FONDECYT N° 1161510 awarded to RC, and by the grant FONDEF ID17I10301 awarded to DEH

Rationale: Cyclic strain may be a determinant of ventilator-induced lung injury. The standard for strain assessment is the computed tomography (CT), which does not allow continuous monitoring and exposes to radiation. Electrical impedance tomography (EIT) is able to monitor changes in regional lung ventilation. In addition, there is a correlation between mechanical deformation of materials and detectable changes in its electrical impedance, making EIT a potential surrogate for cyclic lung strain measured by CT ($Strain_{CT}$).

Objectives: To compare the global $Strain_{CT}$ with the change in electrical impedance (ΔZ).

Methods: Acute respiratory distress syndrome patients under mechanical ventilation (V_T 6 mL/kg ideal body weight with positive end-expiratory pressure 5 [PEEP 5] and best PEEP according to EIT) underwent whole-lung CT at end-inspiration and end-expiration. Biomechanical analysis was used to construct 3D maps and determine $Strain_{CT}$ at different levels of PEEP. CT and EIT acquisitions were performed simultaneously. Multilevel analysis was employed to determine the causal association between $Strain_{CT}$ and ΔZ. Linear regression models were used to predict the change in lung $Strain_{CT}$ between different PEEP levels based on the change in ΔZ.

Main results: $Strain_{CT}$ was positively and independently associated with ΔZ at global level ($P < .01$). Furthermore, the change in $Strain_{CT}$ (between PEEP 5 and Best PEEP) was accurately predicted by the change in ΔZ (R^2 0.855, $P < .001$ at global level) with a high agreement between predicted and measured $Strain_{CT}$.

Conclusions: The change in electrical impedance may provide a noninvasive assessment of global cyclic strain, without radiation at bedside.

Preliminary results were presented in 32nd European Society of Intensive Care Medicine Annual Congress.

1 | INTRODUCTION

Mechanical ventilation is the most important life support in acute respiratory distress syndrome (ARDS), but mechanical ventilation per se may induce lung injury (VILI).[1] Although important advances have been made in the understanding of VILI, the ultimate determinants remain unknown. What is clear is that VILI originates from a mechanical phenomenon.

During the last years, Gattinoni and others have promoted the notion that VILI may be better explained in terms of strain, ie, the relative deformation to which the tissues are subjected.[2-4] The exact measurement of lung strain is still unfeasible in clinical practice, for this reason, lung strain has been considered as the change of volume (tidal volume [V_T]) normalized by a reference volume (functional residual capacity [FRC]).[5] However, as lungs are commonly ventilated with positive end-expiratory pressure (PEEP), a constant basal strain is imposed on them, over which cyclic strain is added by tidal ventilation. There is consistent evidence from mechanical engineering that material fatigue is better explained by accumulated energy due to cyclic loading rather than by static monotonous deformation.[6] This concept is supported by recent data of Protti et al, which show that injury over the lungs is strongly influenced by cyclic strain, even at comparable levels of maximal strain.[7]

Clinical and experimental evidence suggests that certain thresholds of high strain can be associated with lung injury. In mechanically ventilated healthy pigs, using the FRC at Zero End Expiratory Pressure as the reference volume, a level of strain >1.5-2 consistently induced VILI.[7] In a clinical study, by using the end-expiratory lung volume at PEEP (EELV) as the reference volume, strain values above ~0.20 were already enough to promote an inflammatory response characterized by fourfold increase in IL-6 and IL-8 concentrations in bronchoalveolar lavage fluid.[8] In another clinical study using the same reference volume at PEEP, a higher metabolic activity in the ventilated lung was found when strain values were exceeding 0.15-0.2.[9,10]

The best tool available to estimate lung strain is by quantitatively analyzing two computed tomography (CT) scans evaluated at different pressure levels, which is not commonly available at the beside and it exposes the patient to x-ray radiation. In addition, analysis of strain from the CT images still requires intense work, both for the exam and the analysis.[4,11,12]

In this scenario, electrical impedance tomography (EIT) has arisen as a bedside radiation-free functional imaging modality for monitoring lung ventilation and perfusion.[13] Regional impedance changes observed in EIT during tidal ventilation correlate well with changes in absolute air content observed in CT.[14] Recent studies have also suggested an underlying correlation between mechanical deformation of different materials, but also biological tissues, and detectable changes in its electrical impedance.[15-17] Furthermore, the changes in air content and strain are directly related during tidal ventilation, being the former one of the main determinants of the latter.

We hypothesized that changes in electrical impedance can be related to the changes in cyclic lung strain when the level of PEEP is changed. Therefore, the aim of the study was to determine whether EIT monitoring is able to predict changes in cyclic strain in ARDS patients, using CT-based analysis ($Strain_{CT}$) as a benchmark.

Editorial Comment

For ventilator-dependent patients with acute lung injury, attention to avoiding unnecessary lung strain and ventilator-associated lung injury is important. This clinical series shows that electric impedance tomography at the bedside may provide a non-invasive estimation of global lung strain without radiation.

2 | METHODS

To test our hypothesis, we analyzed data obtained from an ongoing clinical study, which included simultaneous acquisitions of CT and EIT (spatially correlated). The study was approved by the Ethics committee for Clinical Studies (No. 027/2016, Hospital Clínico Universidad de Chile).

2.1 | Study protocol

2.1.1 | Study population

Consecutive ICU patients were studied in a university hospital. Informed consent was obtained from the patients' next of kin. The enrolled adult patients fulfilled the criteria for moderate-to-severe ARDS according to Berlin definition.[18] Patients younger than 18 years old, pregnant, with arrhythmias, who had contraindications for installation of EIT, chronic lung diseases or central nervous system injury, or risk of gastric variceal hemorrhage, were excluded. Patients were kept under sedation (Fentanyl and Propofol according to the ICU sedation protocol) plus neuromuscular paralysis (Cisatracurium). They were subjected to a volume-controlled ventilation mode with VT of 6 mL/kg of predicted body weight (Puritan-Bennett 840 Ventilator System—Nellcor Puritan Bennett, CA). Recruitment maneuvers and decremental PEEP titration were used (see below). Patients underwent whole-lung CT, with a low radiation protocol, during breath-holding sessions at end-expiration (EE) and end-inspiration (EI), with PEEP 5 and with best PEEP titrated according to EIT (see Supporting Information). Briefly, best PEEP was defined as the PEEP associated with the lowest combination of collapse and overdistension according to EIT monitoring.

2.1.2 | EIT imaging

EIT was used to visualize the 2D distribution of lung air content during the respiratory cycle (Enlight® 1800; Timpel). The reconstructed

images represent the impedance distribution of each time step of the acquisition series, relative to a convenient reference value taken at the beginning of data acquisition (baseline). The *tidal change in impedance distribution* (ΔZ^{td}, hereafter referred only as ΔZ) was calculated by subtracting EI to EE values. The effect of cardiac cycles on EIT signals was filtered using the mean pletismogram during the respiratory pauses.

2.1.3 | CT imaging

For each PEEP analyzed, two CT scans were acquired in breath-holding sessions during EE and EI phases. The lung geometry was constrained by using a contour-active segmentation (using the software ITK-Snap [Penn Image Computing and Science Laboratory]).[19] Simultaneous acquisition with EIT monitoring allowed to confront these results in the subsequent sections.

2.1.4 | Air content

For both EE and EI respiratory phases, the gas fraction was calculated at voxel level using its corresponding hounsfield units (HU). For each voxel, a linear interpolation was used between HU ≤1000 (100% gas) and HU ≥0 (100% tissue), thus, producing 3D gas fraction maps. Following, the air content was calculated for each voxel by multiplying the gas fraction to the voxel volume.

2.1.5 | Volumetric strain

Volumetric strain (ε_v) corresponds to the local change of volume of the lung parenchyma, which in this study is calculated for a tidal breath. 3D maps of volumetric strain were computed following the image-based biomechanical method.[20,21] In brief, EI and EE images were registered using the Nifty-Reg library,[22] which delivers a transformation between both images. Then, volumetric strain is computed using finite-element projection analysis, which delivers 3D maps of volumetric strain for each patients' lungs (Figure 1). See Supporting Information for a detailed description of the methods. Additional strain analysis, based on the classic approach using V_T divided by EELV, was performed to show the consistency with the finite-element method.

2.1.6 | Spatial correlation between CT and EIT changes

At the beginning of CT, the EIT belt (position) was adjusted so that the plane of the acquired CT slice and EIT signals would match (Figure 2). During CT images acquisitions, EIT was recording the data at the same time, identifying the corresponding CT breath-holding sessions in the EIT time series. Whereas CT reconstruction images

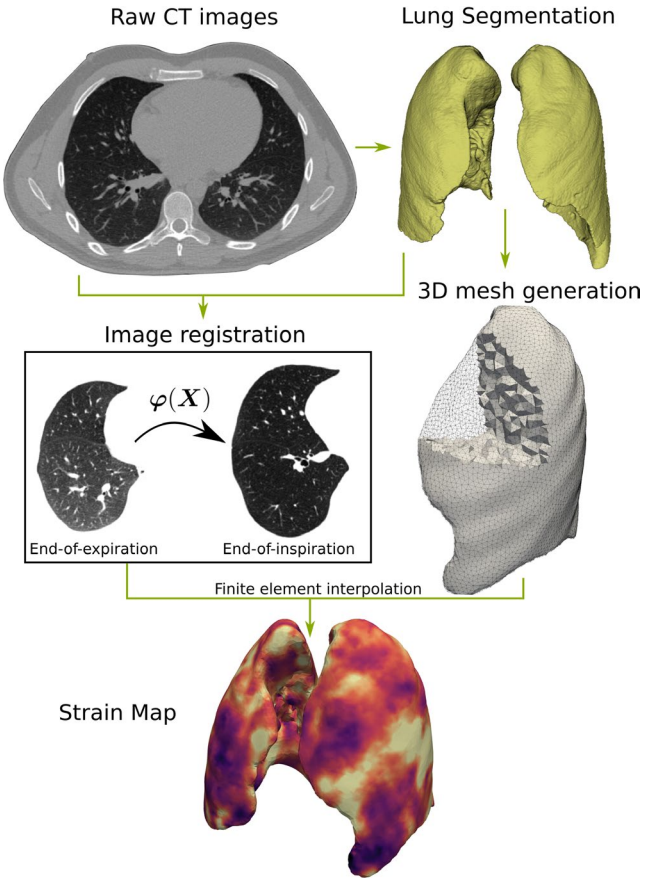

FIGURE 1 Procedure to obtain volumetric strain maps. A segmentation is generated for each end-of-expiration and end-of-inspiration images. Image registration allows to map the deformation between images, followed by projecting these results onto a 3D mesh. CT, computed tomography

produce a 3D map, EIT images represent the impedance values collapsed onto a transverse 2D cross-section, defined by the axial position of the electrode belt along the patient torso. The spatial correspondence between the methods was achieved by integrating $Strain_{CT}$ of the whole lung through an axis perpendicular to the EIT cross-section (ie, the electrode belt identified in the CT image). CT images from both lungs, our region of interest (ROI), were spatially aligned to the regions where ΔZ was calculated for each respiratory phase (Figure 2). Volumetric strain was computed as the average of the regional strain values in each lung in EE. See Supporting Information for a detailed description.

2.2 | Statistical analysis

Normal distribution of data was evaluated by the Shapiro-Wilk test. Continuous data were expressed as mean ± standard deviation or median and interquartile range, meanwhile categorical variables were reported as count and percentage (%). Because repeated measures were done in each ARDS patient (at different PEEP levels), linear mixed-effect models were used to determine the causal association between ΔZ

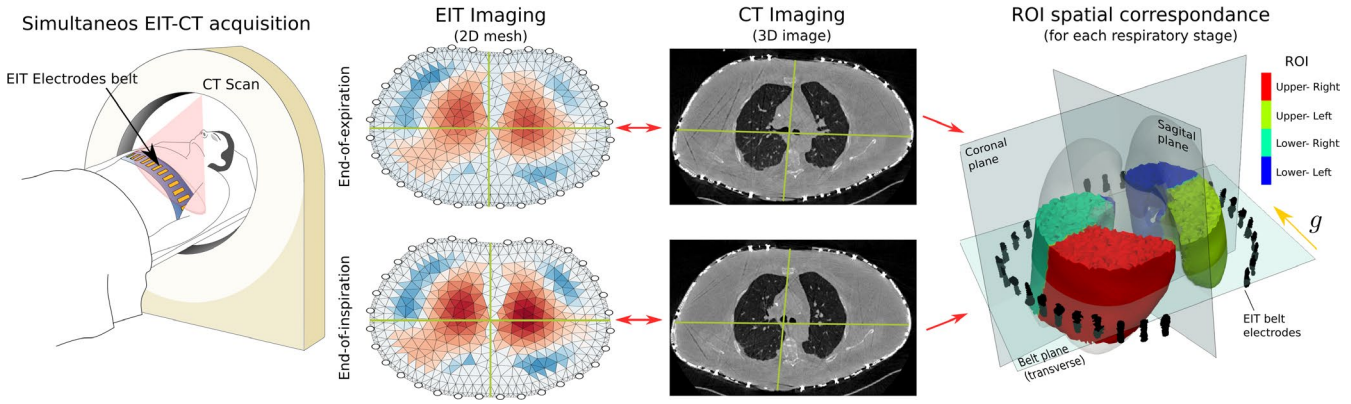

FIGURE 2 Simultaneous EIT and CT data acquisition, sagittal, and coronal planes are obtained to define the ROI that are spatially correspondent. CT, computed tomography; EIT, electrical impedance tomography; ROI, region of interest

obtained by EIT and $Strain_{CT}$, taking into account the patient level as a random effect. To adjust for potential confounders as fixed effects, we used acyclic causal diagrams[23], controlling by body mass index (BMI). Also, we used linear regression models to predict the change in $Strain_{CT}$ between both PEEP levels ($\Delta Strain_{CT}$) based on EIT changes. Finally, diagnostic performance between EIT-based prediction, $\Delta Strain_{EIT}$ with $\Delta Strain_{CT}$, was assessed by Bland-Altman test. Statistical analysis was performed with the software Stata v12.0 (StataCorp), and all graphs were made in Prism 6.0 (GraphPad Software).

3 | RESULTS

We included 13 ARDS patients: age 66 ± 14 years (8 males, 10 medical and 3 surgical admissions, and 5 had primary ARDS); their worst values before the inclusion were as follows: PaO_2/FiO_2 130 ± 38 mm Hg and SOFA 13 ± 4. At the inclusion to the study, the time on mechanical ventilation was 9 ± 5 days, and gas exchange and lung mechanics were already improving in most patients. General characteristics from patients at this phase are shown in Table 1. The values of $Strain_{CT}$, EELV, and ΔZ at global level from ARDS patients are shown in Table 2. The coefficient of determination (R^2) between the two methods to estimate strain (Finite-element method and V_T/EELV) was 0.91 (see Figure S1).

3.1 | Association between $Strain_{CT}$ and EIT

In multilevel analysis, $Strain_{CT}$ was positively associated with ΔZ (Table 3). After adjusting by BMI, an independent association was obtained between $Strain_{CT}$ and ΔZ.

3.2 | Prediction of change in $Strain_{CT}$ ($\Delta Strain_{CT}$) by the change in ΔZ

The change in $Strain_{CT}$ ($\Delta Strain_{CT}$ = [$Strain_{CT}$ at PEEP 5 − $Strain_{CT}$ at Best PEEP]) was predicted by the change in ΔZ (change in ΔZ = [ΔZ at PEEP 5 − ΔZ at Best PEEP]), explaining 86% of the change in $Strain_{CT}$ at global level. Predictive equation for $\Delta Strain_{CT}$ by EIT ($\Delta Strain_{EIT}$) and its R^2 are expressed in Figure 3A.

3.3 | Diagnostic concordance between EIT predictions and $\Delta Strain_{CT}$

Figure 3B shows the diagnostic concordance between ΔEIT predictions through the change in ΔZ ($\Delta Strain_{EIT}$) with $\Delta Strain_{CT}$. A high agreement was observed between $\Delta Strain_{EIT}$ and $\Delta Strain_{CT}$.

A visual comparison between $Strain_{CT}$ and ΔZ, from ARDS patient at PEEP 5 and Best PEEP, is shown in Figure 4. In this example, best PEEP decreased both $Strain_{CT}$ and ΔZ, but also improved lung homogeneity on ventral-to-dorsal distribution.

4 | DISCUSSION

In the present study, a positive and independent association between EIT data (ΔZ) and $Strain_{CT}$ was found in ARDS. In addition, the changes in cyclic strain induced by changes in PEEP were accurately predicted through EIT data, providing a non-invasive surrogate of global cyclic strain without radiation at the bedside.

Imbalances in regional lung ventilation obtained by CT,[14] PET,[24] and MRI[25] (as the validation methods) have been accurately measured by EIT in animal models and humans (with healthy and injured lungs), independently of severity of lung damage or whether breathing was spontaneous or mechanically delivered. Changes in absolute air content best explained impedance changes inside lung regions of interest.[14] However, to the best of our knowledge, this is a first attempt to explore the EIT for lung strain monitoring. Although we obtained good associations and predictions on global lung, more studies are needed to know whether this effect remains significant at regional level, specially at the dependent and non-dependent lung regions, as it is suggested by the visual comparison in Figure 4.

TABLE 1 General characteristics from patients at the inclusion

Patients (number)	Diagnosis	Age (y.o.)	Gender (M/F)	PaO_2/FiO_2 (mm Hg)	PEEP (cmH_2O)	V_T (mL/kg)	DP (cmH_2O)	C_{RS} (mL/cmH_2O)	MV (d)
1	Hemorraghic and septic shock	78	M	253	14	6.1	11	39	9
2	Pulmonary sepsis	77	M	271	10	5.9	8.4	50.5	2
3	Pulmonary sepsis	74	F	234	8	5.9	12.5	19	2
4	Liver transplant/pulmonary Aspergillosis	30	M	216	10	6.2	12	34	20
5	Hemorraghic and septic shock	66	F	284	14	6.2	10	29	13
6	Pulmonary sepsis	75	M	250	12	5.9	9	47.3	16
7	Urinary septic shock	78	F	218	16	5.8	6.6	36	8
8	Abdominal septic shock	75	F	194	12	6.2	10.4	29.8	12
9	Abdominal septic shock	64	M	211	10	6.1	7.9	58.1	4
10	Septic shock	49	F	319	10	6.1	7	52.4	11
11	Liver transplant/septic shock	57	M	236	12	6.2	13	26.9	4
12	Pulmonary sepsis	73	M	292	14	6.0	6	58.3	10
13	Aspirative pneumonia	67	M	186	10	6.0	11	33.6	9

Abbreviations: C_{RS}, compliance of the respiratory system; DP, driving pressure; MV, time on mechanical ventilation at the assessment; PEEP, positive end-expiratory pressure (best PEEP according to EIT is shown in the table); V_T, tidal volume.

TABLE 2 Values of $Strain_{CT}$, EELV, and EIT (ΔZ) at global level in ARDS patients

		Global
$EELV_{CT}$ (L)	PEEP 5	1.140 (1.070-1.151)
	Best PEEP	1.601 (1.478-2.075)
$Strain_{CT}$	PEEP 5	0.232 (0.112-0.273)
	Best PEEP	0.139 (0.109-0.177)
ΔZ_{EIT} (AU)	PEEP 5	30.456 (24.182-33.278)
	Best PEEP	26.768 (20.745-34.372)

Abbreviations: AU, arbitrary units; ARDS, acute respiratory distress syndrome; CT, computed tomography; $EELV_{CT}$, end-expiratory lung volume by CT; EIT, electrical impedance tomography; PEEP, positive end-expiratory pressure; $Strain_{CT}$, strain by computed tomography; ΔZ, electrical impedance change between lung inspiration and expiration.

TABLE 3 Linear association between $Strain_{CT}$ with EIT (ΔZ)

ROI	Crude β (*P*-value)	Adjusted β[a] (*P*-value)
Global	0.032 ($P = .002$)	0.038 ($P < .001$)

Note: β is expressed per 10 units of increment in EIT (ΔZ).

Abbreviations: EIT, electrical impedance tomography; ROI, region of interest; $Strain_{CT}$, strain by computed tomography; ΔZ, electrical impedance change.

[a]β adjusted by end-expiratory lung volume and body mass index (fixed effects) and patient (random effect).

Different strategies have been used to measure FRC (and EELV) and consequently estimate the global strain in knowing the V_T applied. Although CT remains the gold standard for measuring gas lung volume, the helium dilution and the nitrogen dilution techniques are clinically acceptable to measure FRC when applied in patients with a short time constant of the respiratory system.[26] Nevertheless, the CT scan which requires an intense work, both for the test and the analysis, does not allow continuous assessment and exposes to radiation. On the other hand, the helium dilution and the nitrogen dilution techniques require a specific equipment, which only provides the information regarding FRC.

In order to avoid VILI, V_T and PEEP combination needs to be individualized tailoring the ventilatory parameters according to the lung disease and respiratory mechanics, being strain a useful tool. By sizing V_T to individual FRC, lower risks of VILI may be observed.[7,8] In addition, PEEP may recruit previously collapsed alveoli, which become functional but not necessarily strained, or it may increase the strain/stress of previously opened alveoli. For this reason, we decided to calculate strain as V_T/EELV, where EELV includes both FRC and the potential volume recruited by PEEP. This approach does not consider the static component from the numerator, in accordance with the concept that static strain may be less injurious than cyclic strain.[7] Other EIT tools may provide relevant complementary information related to strain in response to PEEP changes, such as overinflation, recruitment, variation in poorly ventilated lung units (silent spaces), and changes on regional inflection points obtained through P-V curves derived by EIT.[27-29] However, these analyses are beyond the scope of current study.

At the same level of PEEP, EIT is measuring the changes in air content during tidal ventilation. When a higher PEEP level is applied, EIT provides the change in end-expiratory lung impedance (related to higher EELV) and the variation in the amplitude of impedance change. In a classical experimental study by Frerichs et al, the authors performed multiple EIT measurements in pigs in three transverse thoracic planes placed around the thorax (at the level of the 3rd, 5th, and 7th intercostal space, respectively) during the

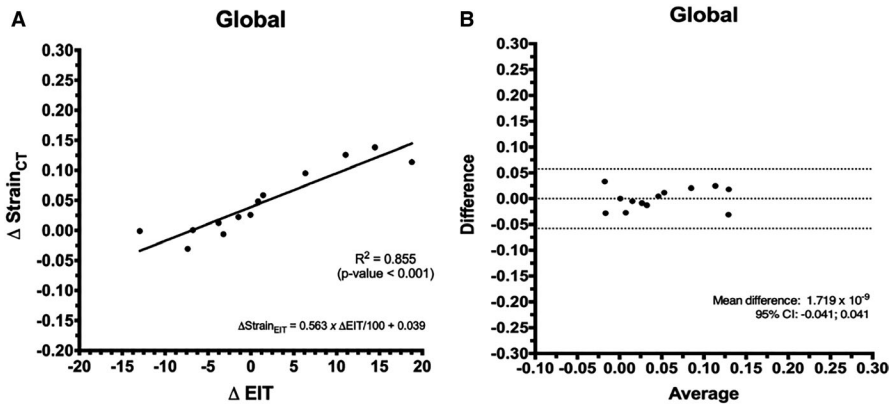

FIGURE 3 Linear regression of change in StrainCT ($\Delta Strain_{CT}$) on change in ΔZ (ΔEIT) is showed in A; and Bland-Altman graph between predicted vs measured $\Delta Strain$, in B. ΔZ, electrical impedance change; EIT, electrical impedance tomography

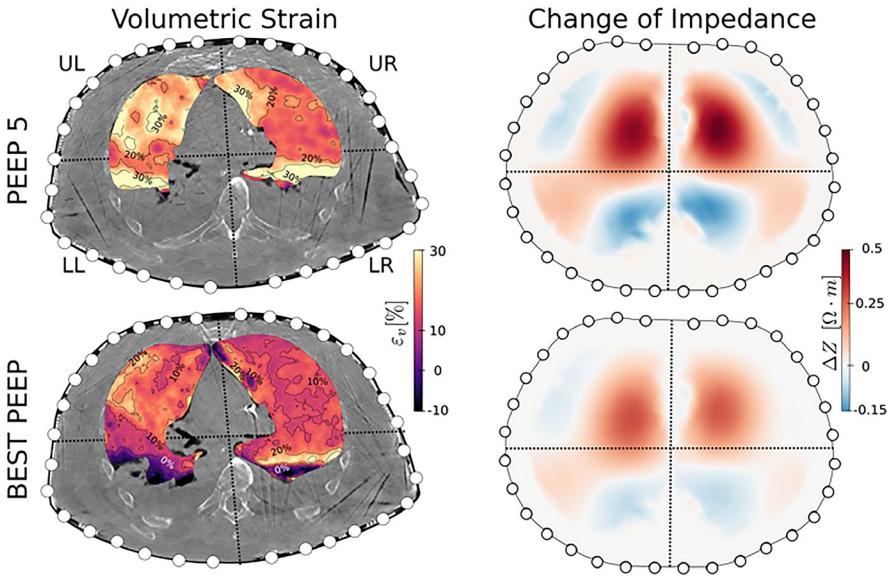

FIGURE 4 Visual comparison between volumetric strain ($Strain_{CT}$) and change of impedance (ΔZ), from ARDS patient at PEEP 5 and Best PEEP. Parallel decrease on these parameters was obtained with the increase in PEEP. ARDS, acute respiratory distress syndrome; PEEP, positive end-expiratory pressure

volume-controlled mode of mechanical ventilation at different V_T and levels of PEEP.[30] In particular, during the variation in PEEP with the same V_T, the determined tidal amplitude of the impedance change (ΔZ) decreased with PEEP in plane 1, was unaffected in plane 2, and increased in plane 3. The authors explained these findings due to the pig thorax anatomy and PEEP-induced lung recruitment. Noteworthy, the authors commented that their preliminary results obtained in humans (in supine positioning) indicated that EIT outputs at different PEEP levels show a decrease in tidal amplitudes of the impedance change in the caudal thoracic plane (plane 3 of their experimental study in pigs).[30] These differences between pigs and human (including our results in ARDS patients with EIT belt at the level of the 5th-6th intercostal space) could be explained by the changes in EELV and strain, although the effect of the out-off plane impedance could also have been present. In our study it was not possible to control the effect of changes in cranial-caudal axis.

In fact, it has recently been suggested an underlying correlation between mechanical deformation of different materials, but also biological tissues, and detectable changes in its electrical impedance.[15-17] In the present study, there was very good correlation and agreement between $Strain_{CT}$ and EIT-predicted models, despite cross-sectional images from EIT represent impedance change in approximately 15-cm-wide slice of the thorax while the $Strain_{CT}$ method is related to the whole lung.[31] The physical properties associated with the deformation have relevance to many physiological, pathological, and clinical processes in mechanically and non-mechanically ventilated patients with acute or chronic lung diseases, which makes EIT a potentially useful tool for patient-tailored treatment.

4.1 | Weakness and strengths

We acknowledge that the relatively small sample size is one of the main limitations of the study. However, it has recently been proposed for linear regression models that only two subjects per variable are required for adequate estimation of regression coefficients, standard errors, and confidence intervals.[32] Nevertheless, further experimental and clinical studies are warranted in order to confirm our observations in larger cohorts and also in ARDS patients at the onset of mechanical ventilation.

Strain monitoring for both methods, finite element and the ratio of V_T to EELV, was comparable. Although strain threshold able to damage baby lung using EELV as the reference volume was reached (ie, strain values above ~0.20), we did not measure neither

biomarkers nor metabolic activity in the ventilated lung; our aim was to test if EIT monitoring is able to predict the changes in global cyclic strain when we increase the level of PEEP. In addition, global strain does not capture the inherent heterogeneity in lung deformation, where regional strain amplifications usually arise,[20,21,33,34] which may be obtained using strain based on biomechanical CT method. Finite-element method was performed for this complementary analysis. Future research should include a broader group of ARDS patients to estimate regional strain employing these methods, and the effect of V_T and PEEP at regional level.

Multilevel analyses in this clinical-physiological scenario are still rare but necessary to evaluate effects of individual-level (repeated measures) and group-level factors. $Strain_{CT}$ and EIT variables were measured more than once for each subject. Therefore, data contain natural clusters, the independence assumption cannot be applied to the observations, and intracluster correlation must be considered in the association between EIT data (ΔZ) and CT data ($Strain_{CT}$) by EIT-based models.[35,36] However, to obtain a reliable and feasible way to estimate the changes in $Strain_{CT}$ from EIT variables in clinical practice, we performed a traditional linear model, subtracting repeated measures, and subsequently, removing the clustered structure of data. Predictions of changes in $Strain_{CT}$ by EIT model in linear regression were very good and accurate.

The aim of this study is not to replace the CT for ARDS lung assessment, but rather to provide evidence for an alternative tool provided by EIT having in mind the CT findings. The synergy between CT and EIT to monitor ARDS patients is expected to grow in the years to come. Even more, the concept of complementarity between CT and EIT has been recently explored using phantoms through a ROI co-registration fusion algorithm.[37] Surrogates of VILI defined by CT analysis have a significantly higher specificity and precision, but EIT can take advantage of being a radiation-free method available at bedside, as well as by providing continuous assessment of respiratory status. Moreover, in addition to the potential estimation of strain by ΔZ, EIT monitoring gives also information about ventilation heterogeneity, the pendelluft phenomenon, and pulmonary perfusion, among others, which increases the clinical utility of EIT at bedside.[38]

Under low tidal volume strategy, we could obtain a good correlation and agreement between the changes in strain and the changes in ΔZ induced by PEEP. This is an important finding because a protective strategy may not ensure lung protection for all ARDS patients if the PEEP level set is inappropriate.[39,40] In some of our patients, a markedly decreased strain was observed after PEEP increment (from PEEP 5 to Best PEEP; Figure 4). Continuous monitoring of cyclic strain could provide relevant information to avoid VILI; through EIT, changes in lung cyclic strain can become clinically available.

5 | CONCLUSION

Our findings suggest that EIT may provide a non-invasive estimation of global lung strain without radiation at the bedside. Assessing strain EIT-based, lung protective ventilation strategies may be tailored; however, future studies are needed to confirm this assumption.

AUTHORS' CONTRIBUTIONS

RC, PI, TM, CK: Substantial contributions to conception and design. RC, PI, TO, CK, DA, DG, MAC, RB, ML, LL, CM, SG, MZ, VR, JNM, CR, DEH: Acquisition of data. RC, PI, TO, CK, DA, AIJG, CM, DEH, AB: Analysis and interpretation of data. RC, PI, TO, CK, DA, DG, MAC, RB, AIJG, ML, CM, LL, SG, MZ, VR, JNM, CR, DEH, AB: Drafting the article or revising it critically for important intellectual content. RC, PI, TO, CK, DA, DG, MAC, RB, AIJG, ML, CM, LL, SG, MZ, VR, JNM, CR, DEH, AB: Final approval of the version to be published.

ORCID

Rodrigo Cornejo https://orcid.org/0000-0002-0497-5740

REFERENCES

1. Slutsky AS, Ranieri VM. Ventilator-induced lung injury. *N Engl J Med*. 2013;369:2126-2136.
2. Gattinoni L, Carlesso E, Cadringher P, Valenza F, Vagginelli F, Chiumello D. Physical and biological triggers of ventilator-induced lung injury and its prevention. *Eur Respir J*. 2003;22:15s-25s.
3. Gattinoni L, Caironi P, Carlesso E. How to ventilate patients with acute lung injury and acute respiratory distress syndrome. *Curr Opin Crit Care*. 2005;11:69-76.
4. Protti A, Cressoni M, Santini A, et al. Lung stress and strain during mechanical ventilation: any safe threshold? *Am J Respir Crit Care Med*. 2011;183:1354-1362.
5. Chiumello D, Carlesso E, Cadringher P, et al. Lung stress and strain during mechanical ventilation for acute respiratory distress syndrome. *Am J Respir Crit Care Med*. 2008;178:346-355.
6. Lazzeri A, Marchetti A, Levita G. Fatigue and fracture in polyacetal resins. *Fatigue Fract Eng Mater Struct*. 1997;20:1207-1216.
7. Protti A, Andreis DT, Monti M, et al. Lung stress and strain during mechanical ventilation: any difference between statics and dynamics? *Crit Care Med*. 2013;41:1046-1055.
8. González-López A, García-Prieto E, Batalla-Solís E, et al. Lung strain and biological response in mechanically ventilated patients. *Intensive Care Med*. 2012;38:240-247.
9. Bellani G, Guerra L, Musch G, et al. Lung regional metabolic activity and gas volume changes induced by tidal ventilation in patients with acute lung injury. *Am J Respir Crit Care Med*. 2011;183:1193-1199.
10. Wellman TJ, Winkler T, Costa ELV, et al. Effect of local tidal lung strain on inflammation in normal and lipopolysaccharide-exposed sheep. *Crit Care Med*. 2014;42:e491-e500.
11. Gattinoni L, Caironi P, Valenza F, Carlesso E. The role of CT-scan studies for the diagnosis and therapy of acute respiratory distress syndrome. *Clin Chest Med*. 2006;27:559-570.
12. Caironi P, Cressoni M, Chiumello D, et al. Lung opening and closing during ventilation of acute respiratory distress syndrome. *Am J Respir Crit Care Med*. 2010;181:578-586.
13. Frerichs I, Amato MBP, Van Kaam AH, et al. Chest electrical impedance tomography examination, data analysis, terminology, clinical use and recommendations: Consensus statement of the TRanslational EIT developmeNt stuDy group. *Thorax*. 2017;72:83-93.
14. Victorino JA, Borges JB, Okamoto VN, et al. Imbalances in regional lung ventilation: a validation study on electrical impedance tomography. *Am J Respir Crit Care Med*. 2004;169:791-800.

15. Hou T-C, Lynch JP. Electrical impedance tomographic methods for sensing strain fields and crack damage in cementitious structures. *J Intel Mater Syst Struct*. 2009;20:1363-1379.
16. Tallman TN, Wang KW. Damage and strain identification in multifunctional materials via electrical impedance tomography with constrained sine wave solutions. *Struct Heal Monit*. 2016;15:235-244.
17. Belmont B, Dodde RESA, Shih AJ. Impedance of tissue-mimicking phantom material under compression. *J Electr Bioimp*. 2019;4:2-12.
18. Ranieri VM, Rubenfeld GD, Thompson BT, et al. Acute respiratory distress syndrome: the Berlin definition. *J Am Med Assoc*. 2012;307:2526-2533.
19. Yushkevich PA, Piven J, Hazlett HC, et al. User-guided 3D active contour segmentation of anatomical structures: significantly improved efficiency and reliability. *NeuroImage*. 2006;31:1116-1128.
20. Hurtado DE, Villarroel N, Retamal J, Bugedo G, Bruhn A. Improving the accuracy of registration-based biomechanical analysis: a finite element approach to lung regional strain quantification. *IEEE Trans Med Imaging*. 2016;35:580-588.
21. Hurtado DE, Villarroel N, Andrade C, Retamal J, Bugedo G, Bruhn A. Spatial patterns and frequency distributions of regional deformation in the healthy human lung. *Biomech Model Mechanobiol*. 2017;16:1413-1423.
22. Modat M, Ridgway GR, Taylor ZA, et al. Fast free-form deformation using graphics processing units. *Comput Methods Programs Biomed*. 2010;98:278-284.
23. Lederer DJ, Bell SC, Branson RD, et al. Control of confounding and reporting of results in causal inference studies. guidance for authors from editors of respiratory, sleep, and critical care journals. *Ann Am Thorac Soc*. 2019;16:22-28.
24. Richard J, Pouzot C, Gros A, et al. Electrical impedance tomography compared to positron emission tomography for the measurement of regional lung ventilation: an experimental study. *Crit Care*. 2009;13:R82.
25. Dunster KR, Friese MEJ, Fraser JF, Galloway GJ, Cowin GJ, Schibler A. Ventilation distribution in rats: part 2—a comparison of electrical impedance tomography and hyperpolarised helium magnetic resonance imaging. *Biomed Eng Online*. 2012;11:68.
26. Chiumello D, Cressoni M, Chierichetti M, et al. Nitrogen washout/washin, helium dilution and computed tomography in the assessment of end expiratory lung volume. *Crit Care*. 2008;12:R150.
27. Songqiao Liu S, Tan L, Möller K, et al. Identification of regional overdistension, recruitment and cyclic alveolar collapse with electrical impedance tomography in an experimental ARDS model. *Crit Care*. 2016;20:119.
28. Spadaro S, Mauri T, Böhm SH, et al. Variation of poorly ventilated lung units (silent spaces) measured by electrical impedance tomography to dynamically assess recruitment. *Crit Care*. 2018;22:26.
29. Scaramuzzo G, Spadaro S, Waldmann AD, et al. Heterogeneity of regional inflection points from pressure-volume curves assessed by electrical impedance tomography. *Crit Care*. 2019;23:119.
30. Frerichs I, Hahn G, Hellige G. Thoracic electrical impedance tomographic measurements during volume controlled ventilation-effects of tidal volume and positive end-expiratory pressure. *IEEE Trans Med Imaging*. 1999;18:764-773.
31. Costa ELV, Lima PG, Amato MBR. Electrical impedance tomography. *Curr Opin Crit Care*. 2009;15:18-24.
32. Austin PC, Steyerberg EW. The number of subjects per variable required in linear regression analyses. *J Clin Epidemiol*. 2015;68:627-636.
33. Cressoni M, Cadringher P, Chiurazzi C, et al. Lung inhomogeneity in patients with acute respiratory distress syndrome. *Am J Respir Crit Care Med*. 2014;189:149-158.
34. Sarabia-Vallejos MA, Zuñiga M, Hurtado DE. The role of three-dimensionality and alveolar pressure in the distribution and amplification of alveolar stresses. *Sci Rep*. 2019;9(1):8783.
35. Bangdiwala SI. The multilevel diagram. *Int J Inj Contr Saf Promot*. 2012;19:388-390.
36. De Livera AM, Zaloumis S, Simpson JA. Models for the analysis of repeated continuous outcome measures in clinical trials. *Respirology*. 2014;19:155-161.
37. Schullcke B, Gong B, Krueger-Ziolek S, Soleimani M, Mueller-Lisse U, Moeller K. Structural-functional lung imaging using a combined CT-EIT and a discrete cosine transformation reconstruction method. *Sci Rep*. 2016;6:25951.
38. Tomicic V, Cornejo R. Lung monitoring with electrical impedance tomography: technical considerations and clinical applications. *J Thorac Dis*. 2019;11(7):3122-3135.
39. Grasso S, Stripoli T, De Michele M, et al. ARDSnet ventilatory protocol and alveolar hyperinflation: Role of positive end-expiratory pressure. *Am J Respir Crit Care Med*. 2007;176:761-767.
40. Terragni PP, Rosboch G, Tealdi A, et al. Tidal hyperinflation during low tidal volume ventilation in acute respiratory distress syndrome. *Am J Respir Crit Care Med*. 2007;175:160-166.

SUPPORTING INFORMATION

Additional supporting information may be found online in the Supporting Information section.

How to cite this article: Cornejo R, Iturrieta P, Olegário TMM, et al. Estimation of changes in cyclic lung strain by electrical impedance tomography: Proof-of-concept study. *Acta Anaesthesiol Scand*. 2020;00:1–8. https://doi.org/10.1111/aas.13723